nature geoscience

ARTICLES

PUBLISHED ONLINE: 18 SEPTEMBER 2017 | DOI: 10.1038/NGEO3030

# Earth's early $O_2$ cycle suppressed by primitive continents

Matthijs A. Smit[1]* and Klaus Mezger[2]

**Free oxygen began to accumulate in Earth's surface environments between 3.0 and 2.4 billion years ago. Links between oxygenation and changes in the composition of continental crust during this time are suspected, but have been difficult to demonstrate. Here we constrain the average composition of the exposed continental crust since 3.7 billion years ago by compiling records of the Cr/U ratio of terrigenous sediments. The resulting record is consistent with a predominantly mafic crust prior to 3.0 billion years ago, followed by a 500- to 700-million-year transition to a crust of modern andesitic composition. Olivine and other Mg-rich minerals in the mafic Archaean crust formed serpentine minerals upon hydration, continuously releasing $O_2$-scavenging agents such as dihydrogen, hydrogen sulfide and methane to the environment. Temporally, the decline in mafic crust capable of such process coincides with the first accumulation of $O_2$ in the oceans, and subsequently the atmosphere. We therefore suggest that Earth's early $O_2$ cycle was ultimately limited by the composition of the exposed upper crust, and remained underdeveloped until modern andesitic continents emerged.**

The first profound rise of atmospheric oxygen levels occurred during a period known as the Great Oxidation Event (GOE, 2.4–2.2 Gyr ago[1,2]). The GOE is marked by an abrupt disappearance of mass-independent S isotope fractionation from the rock record 2.32 Gyr ago[3] (Fig. 1a). Low-level $O_2$ accumulation in the shallow oceans commenced at least 300 Myr earlier, as evidenced by the Mo (ref. 4), Cr (ref. 5), and Fe (ref. 6) isotope records of banded iron formations (BIF, Fig. 1b,c) and the geochemistry of platform-facies black shales[7]. Oxygen saturation of soils is traced back even further (2.99 Gyr ago[8]). The development of an $O_2$ cycle is ultimately ascribed to the emergence of cyanobacteria, which occurred sometime during the Mesoarchaean era[6]. Substantial uncertainty exists as to why oxygenation was slow and stepwise, rather than fast and continuous. Recent studies on Archaean rocks suggest that oxygenation was suppressed pending a secular change in the composition of the continental crust[9–11]. Such a change may have caused a decline in Ni supply to the oceans, thus decreasing methanogen proficiency[9,12], or could have lowered the $O_2$-buffer capacity of subaerial weathering[11]. Either concept would be supported by the growth of exposed felsic crust since 3.3 Gyr ago[13], and systematic changes in Ni/Fe of Neoarchaean BIF and Cr/Zn of global shales[12,14] (Fig. 1d).

Reliable and representative constraints on the composition of the Archaean upper continental crust (UCC) are needed to elucidate possible links with Earth's $O_2$ cycle. The Archaean crust may have been compositionally mixed and density unstable, with mafic upper crust, formed by volcanic surfacing, overlying a more andesitic middle crust[15]. A more mafic upper crust is consistent with the general dearth of zircon in Archaean sediments[16]. Nevertheless, uncertainty remains because preserved fragments of Archaean crust are scarce and were possibly subject to reworking and preservation bias[17]. Terrigenous sedimentary rocks such as shales provide an opportunity to provide a more representative picture of the Archaean crust. Such rocks sample large catchments within the subaerial UCC, and hence permit representative constraints on average composition of this reservoir through time[14,18–20]. Compositional bias in sediments relative to source rocks can be effectively circumvented using robust elemental proxies[14,20,21]. Following such an approach, we focus on Cr/U. This elemental ratio provides a useful proxy for silicate differentiation in Earth's mantle and crust, because U is highly incompatible and Cr in its common trivalent state is not. The ratio has two advantages for use as a tracer for sedimentary protolith: Cr and U are both hosted in refractory detrital minerals—for example, chromite and clinopyroxene (Cr), and zircon (U)—and both species are fluid-immobile unless subjected to oxidative weathering, which produces soluble (hydro)chromate [$Cr(VI)O_4^{2-}$, $HCr(VI)O_4^-$] (ref. 5) and uranyl [$U(VI)O_2^{2+}$] (ref. 21). The latter indicates that Cr/U may not be fractionated during weathering, either because Cr and U are bound to refractory minerals and decoupled from major elements (reduced environment) or because they are equally removed (oxidized environment). Fractionation of Cr/U may be expected only in cases where Cr and U are not equally oxidized during weathering, or are hosted in minerals with greatly different solubility. The latter may occur if Cr is hosted by chromite, which shows a solubility that is strongly pH-dependent[22] and probably higher than that of zircon. Vice versa, U may be preferentially lost from highly oxidized detritus in which soluble uraninite is the main U carrier. The net effect of such preferential weathering on Cr/U is difficult to predict. Nevertheless, if significant, this effect should increase with the degree of weathering, and can hence be tested for by comparing Cr/U and the degree of weathering, commonly quantified through the chemical index of alteration [CIA; molar $Al_2O_3/(Al_2O_3 + CaO + Na_2O + K_2O)$]. Assuming that weathering conditions were similar across sedimentary catchments, this test would also be valid for cases of pre-depositional weathering.

Values of Cr/U relative to a modern standard are expressed as $\Delta$(Cr/U), which is defined as $[\ln(Cr/U)/\ln(Cr/U)_{PAAS}]$-1 (PAAS = Post-Archaean Australian Shale; data in Supplementary Table 1). Sensitivity of Cr/U to silicate differentiation is shown by the consistent decrease in $\Delta$(Cr/U) trends with $SiO_2$ for components of Earth's crust and mantle (Fig. 2a and Supplementary Fig. 1). Average $\Delta$(Cr/U) values for mantle rocks (for example, lherzolite = $2.0 \pm 0.6$) and mid-oceanic ridge basalts (MORB = $1.3 \pm 0.2$)

[1]Department of Earth, Ocean and Atmospheric Sciences, University of British Columbia, 2020-22017 Main Mall, Vancouver V6T 1Z4, Canada. [2]Institut für Geologie, Universität Bern, Baltzerstrasse 1+3, CH-3012 Bern, Switzerland. *e-mail: msmit@eoas.ubc.ca

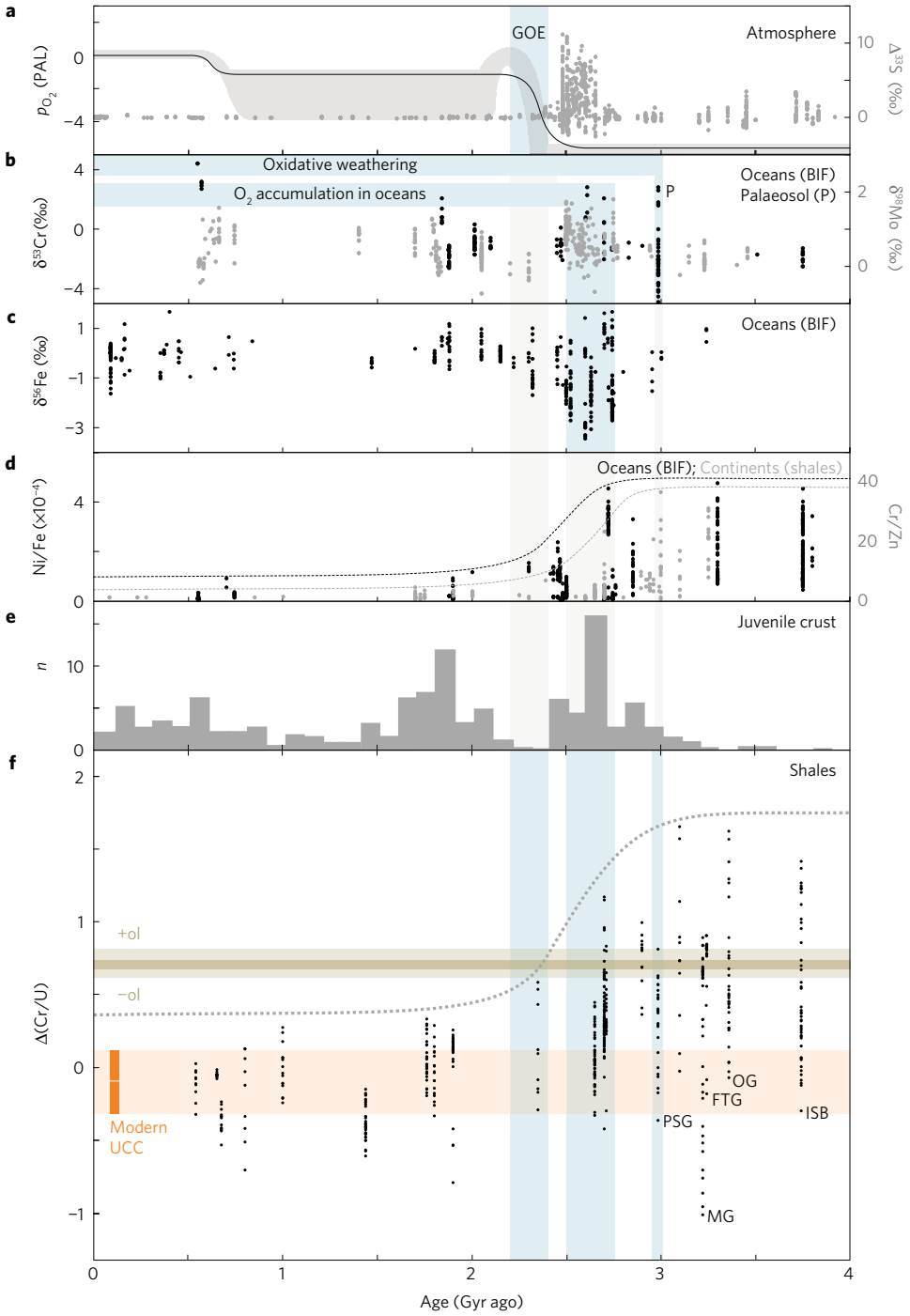


**Figure 1 | Time evolution of oxygenation and crustal evolution. a**, Models for atmospheric oxygen levels relative to present day (PAL)[2] with $\Delta^{33}S$ data[3]. **b**,**c**, Oceanic $O_2$ accumulation commenced 0.3 Gyr before the GOE, as shown by Mo (ref. 4), Cr (ref. 5) (**b**) and Fe (ref. 6) (**c**) isotope data from BIF. **d**,**e**, Shale Cr/Zn and BIF Ni/Fe indicate an evolution towards felsic crust since 3.0 Gyr ago (**d**), consistent with the rise in the number ($n$) of known complexes of juvenile crust[13] (**e**). **f**, Δ(Cr/U) of shales. Labels: Pongola Supergroup (PSG), Moodies Group (MG), Fig Tree Group (FTG), Onverwacht Group (OG) and the Isua Supracrustal Belt (ISB).

are significantly higher than those of the modern bulk continental crust (BCC = 0.2 ± 0.1) and the UCC (−0.1 ± 0.2), and are exponentially correlated with olivine content as calculated using the Cross–Iddings–Pirsson–Washington (CIPW) Norm (Supplementary Fig. 1). A similar systematic is observed when evaluating all Cr/U data ($n > 48{,}000$) available for rocks in the international rock database (Fig. 2b, data in Supplementary Fig. 2, and Supplementary Tables 2 and 3). Specifically, this database allows distinction regarding the stability of olivine (ol) and orthopyroxene (opx). A Δ(Cr/U) value of 0.7 consistently distinguishes between rocks that contain these minerals and rocks that do not. The value represents the limit for picritic basalt [primitive ol- and opx-bearing basalt; Δ(Cr/U) = 1.4 ± 0.7] and andesite proper [ol-free and opx-poor or -absent andesite; Δ(Cr/U) = −0.1 ± 0.8].

## Cr/U record of crustal evolution

Shales from various locations and of different depositional age were investigated for their Δ(Cr/U) composition (Fig. 1f). A broad trend

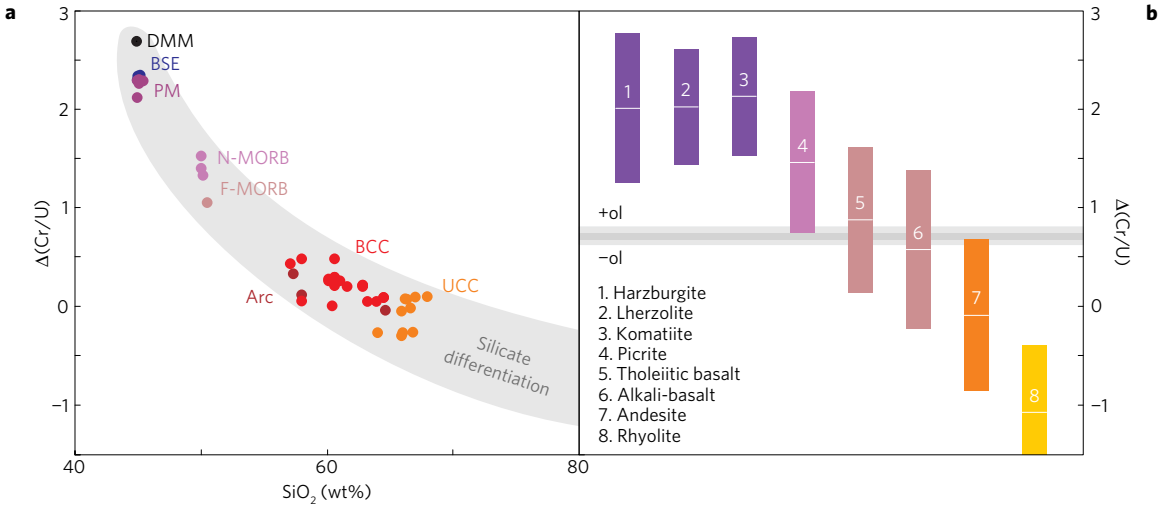


**Figure 2 | Cr/U of major terrestrial reservoirs and rock types. a**, Δ(Cr/U) versus $SiO_2$ showing Cr/U fractionation by silicate differentiation. BCC, bulk continental crust; Arc, oceanic and island arcs; F-MORB, fresh mid-oceanic ridge basalt; N-MORB, normal MORB; PM, primitive mantle; BSE, modelled bulk silicate Earth; DMM, depleted MORB mantle. **b**, Δ(Cr/U) for various rock types. Bars represent average (white line) and 2$\sigma$ based on $n = 629$ (1), 350 (2), 508 (3), 654 (4), 2,776 (5), 17,776 (6), 3,386 (7) and 3,888 (8). Light-grey bar marks the margin between 95% of picrite and andesite data.

with time is identified in the Cr/U systematics of these shales: Δ(Cr/U) values for the past 2.0 Gyr closely approximate that of the modern crust, whereas older shales show higher and more variable Δ(Cr/U). Maximum Δ(Cr/U) values [$\Delta(Cr/U)^{max}$] are highest for the 3.74-Gyr-old Isua shales—one of the oldest sedimentary strata on Earth—and are lower for younger sediments. Values of Δ(Cr/U) do not correlate with CIA for any of the given samples (Supplementary Fig. 3). This indicates that the weathering and alteration of samples—substantial in many cases—did not significantly fractionate or bias Δ(Cr/U) relative to the source signature. This applies to all shale occurrences, regardless of whether they were deposited before or after the GOE. Bias may be introduced by preferential erosion of mafic rocks relative to more felsic lithologies such as granitoids. Although this effect may skew the Δ(Cr/U) dataset, it cannot shift Δ(Cr/U) values beyond the range present among the source rocks. The Δ(Cr/U) values thus trace reliably the composition and chemical heterogeneity of shale detritus and the local UCC from which it was derived.

The Δ(Cr/U) values for shales indicate little or no compositional change within the UCC since 2.0 Gyr ago. A dearth of known shale occurrences deposited 2.5–2.0 Gyr ago impedes insight into the immediate period of the GOE. Still, it is clear that shales deposited before this period—and particularly before 3.0 Gyr ago—have distinctly higher Δ(Cr/U) values. The data indicate that the Archaean UCC was compositionally relatively heterogeneous and—in addition to abundant intermediate and felsic rocks—contained rocks with substantial amounts of ol. This is consistent with the observed lithological diversity of Archaean greenstone belts[15] and provides nuance beyond the general view that Archaean UCC was relatively mafic[14,20,23].

The loss of shales indicating ol-bearing sources occurred during or shortly after the Mesoarchaean, which is widely regarded as an era of enhanced crustal growth through the widespread formation of tonalite–trondhjemite–granite (TTG) complexes[15,23]. The mechanism driving this growth is still debated, and could mark the start of plate tectonics[14,23,24] or the removal of a thermal boundary layer within the mantle[15]. Regardless of the mechanism, the new TTG-type crust diluted below significance the ol-bearing portion of the UCC, possibly by substituting for it or by emerging more extensively above sea level[25]. Although this crustal transformation was possibly part of a global secular change[14,15,23,24], it may have been neither globally synchronous nor locally uniform. In fact, $\Delta(Cr/U)^{max}$ values vary greatly 3.2–2.4 Gyr ago, even for the Barberton shales, which are of similar age and palaeogeography. Conservatively, we can conclude that crustal transformation was first recorded locally in the granite-, dacite- and andesite-sourced[26,27] shales of the 3.2-Gyr-old Moodies and Fig Tree Groups (Fig. 1f), and was globally completed 2.0 Gyr ago.

## $O_2$ scavenging by the Archaean continental crust

The following three observations indicate a profound link between the fate of the primitive mafic rocks among the UCC and the accumulation of $O_2$ in the oceans and atmosphere: there was no significant $O_2$ accumulation in the oceans when these rocks were still abundant[28]; the decline of these rocks among the subaerial UCC was synchronous with the accumulation of organic matter and $O_2$ in the oceans 3.0–2.5 Gyr ago[2,4–7,29]; and removal of these rocks was rapidly succeeded by the GOE (Fig. 1f). These observations indicate that the development of Earth's $O_2$ cycle was limited not by the production of $O_2$ in the cyanobacterial habitat, but rather by the dominantly mafic composition of the Archaean continents. This limiting effect is generally ascribed to an Fe-enriched Archaean UCC, which released more $Fe^{2+}$ in the environment[11]. We, however, find that high Δ(Cr/U) values do not necessarily imply that rocks have high Fe concentrations. All rocks with Δ(Cr/U) between 0.4–2.0 are some variety of basalt, which—although different in $SiO_2$ and ol content—show similar Fe concentrations ([Fe]; 0.7–1 wt%; Supplementary Fig. 4) and $Fe^{3+}/Fe^{total}$ (0.12–0.18; ref. 30). Hence, the loss of rocks with Δ(Cr/U) above 0.7 does not imply that Fe-rich rocks disappeared from the UCC; they, in fact, persisted at least until the GOE. Vice versa, if Fe concentrations did decline during the period of oxygenation, this compositional change alone cannot explain why ΔCr/U of shales decreased. A decline in [Fe] is an inevitable result of crustal transformation and may have aided oxygenation[11]. Still, we require an alternative mechanism that links the loss of ol-bearing rocks to weakening of the $O_2$ buffer of surface waters.

The Δ(Cr/U) data uniquely show that ol- and opx-bearing lithologies were a major component of the Archaean UCC. This mafic to ultramafic Archaean UCC underwent serpentinization wherever rocks interacted with deep hydrothermal fluids and $H_2O$ released from buried hydrous rocks. We propose here that this

process controlled transient suppression of $O_2$ accumulation in the Archaean environment and oceans. Serpentinization involves a series of reactions that ultimately transforms ol and opx into chrysotile (serpentine; srp), brucite (brc), talc (tlc), and magnetite (mgt). The governing reactions are summarized into balanced reactions (1) and (2), which apply to silica-undersaturated systems with different Mg# for ol and opx at low temperature (<300 °C) (refs 31,32). The reactions produce $H_2$, which triggers hydrosynthetic reactions, including pure hydrosynthesis (3), the reaction of $SO_2$ to $H_2S$ (4), and Fischer–Tropsch-type synthesis of $CH_4$ from CO and $CO_2$ (5) (refs 10,31,33–35). As a result of these reactions, surface waters in regions of active low-temperature serpentinization are hyper-alkaline (pH = 10–13) and extremely enriched in $O_2$ scavengers such as $H_2$, $H_2S$, $HS^-$, and $CH_4$ (refs 31,35). In the present-day UCC, ol-bearing rocks are rare and hyper-alkaline waters occur only locally[35]. Before 3.0 Gyr ago, however, such rocks were common to the extent that some shale catchments showed an average modal ol abundance of 15–20 wt%. Thus, surface waters that are now considered extreme in terms of alkalinity were common among surface environments, including the cyanobacterial habitat (for example, soils, lakes, estuaries and continental-shelf waters). Removal of the $O_2$ scavengers from this habitat between 3.0–2.4 Gyr ago would have raised the $O_2$ flux and $Fe^{3+}/Fe^{total}$ of continental runoff. It is hence this cleansing that could explain the first occurrence of $O_2$ accumulation in the surface waters at the time[4–7,29].

$$6\mathrm{ol} + (8x+1)\mathrm{H_2O} \rightarrow 3\mathrm{srp} + 3(4x-3)\mathrm{brc} + 4(1-x)\mathrm{mgt} + 4(1-x)\mathrm{H_2} \quad x = \mathrm{Mg\#(ol)} \tag{1}$$

$$6\mathrm{opx} + 3(1-y)\mathrm{brc} + (1+2y)\mathrm{H_2O} \rightarrow \mathrm{tlc} + \mathrm{srp} + (1-y)\mathrm{mgt} + (1-y)\mathrm{H_2} \quad y = \mathrm{Mg\#(opx)} \tag{2}$$

$$2\mathrm{H_2} + \mathrm{O_2} \rightarrow 2\mathrm{H_2O} \tag{3}$$

$$3\mathrm{H_2} + \mathrm{SO_2} \rightarrow \mathrm{H_2S} + \mathrm{H_2O} \tag{4}$$

$$4\mathrm{H_2} + \mathrm{CO_2} \rightarrow \mathrm{CH_4} + 2\mathrm{H_2O} \tag{5}$$

The importance of serpentinization within the UCC could be scrutinized, considering that the $H_2$ flux from this process was possibly dwarfed by that of seafloor serpentinization. With the latter processes remaining active, it could be expected that $O_2$ escaping scavenging within the UCC would be lost to this persistent $O_2$ buffer unless the seafloor itself underwent a fundamental change[10]. We note, however, that the Archaean ocean was strongly stratified, and the deep ocean remained largely isolated and anaerobic until well after the GOE[2,36]. This indicates that neither $O_2$ accumulation in the oceans nor the GOE were inhibited by seafloor serpentinization or any steady loss of $O_2$ that it may have caused. The $O_2$ saturation required to explain oxygenation must have depended largely, if not entirely, on $O_2$ supply outpacing the ongoing loss to shallow sinks (for example, oxidation of organic matter and $Fe^{2+}$ in rivers and oceans). From the similar timing of the GOE and disappearance of ol among the UCC (Fig. 1f), it would appear that the shallow oceans reached $O_2$ saturation when serpentinization within the UCC ultimately stagnated and continents developed modern andesitic compositions.

This study reports and explains the synchronicity between a changing crustal composition, and the accumulation of $O_2$ in the oceans and atmosphere during the Precambrian. By highlighting the role of serpentinization, our model provides new and important mechanistic insights into the link between continental evolution and global oxygenation. The model moves beyond the general concept that this link is controlled by the Fe concentration of rocks[11], and could explain global oxygenation without requiring wholesale $H_2$ escape and mantle oxidation[37], or a decline in submarine volcanism[38]. The validity of this model can be tested through its predictions. One is that early $O_2$ oases are expected to have developed in regions where mafic rocks were removed early or were altogether lacking. Observations from the Pongola Group could support this. The Pongola Group is the location where first known occurrences of subaerial oxidative weathering[8] and $O_2$-bearing near-shore ocean waters[29] were discovered. Consistent with these early signals of oxygenation, the shales of this group are characterized by low Δ(Cr/U). The Cr/U data would thus indicate that $O_2$ oases occurred since 3.2 Gyr ago, and Earth's surface environments were heterogeneously oxidized during the 0.8 Gyr that followed.

## Methods

Methods, including statements of data availability and any associated accession codes and references, are available in the online version of this paper.

Received 4 March 2017; accepted 22 August 2017; published online 18 September 2017

## References


1. Canfield, D. E. The early history of atmospheric oxygen. *Annu. Rev. Earth Planet. Sci.* **33,** 1–36 (2005).
2. Lyons, T. W., Reinhard, C. T. & Planavsky, N. J. The rise of oxygen in Earth's early ocean and atmosphere. *Nature* **506,** 307–315 (2014).
3. Farquhar, J., Bao, H. & Thiemens, M. Atmospheric influence of Earth's earliest sulfur cycle. *Science* **289,** 756–759 (2000).
4. Anbar, A. D. *et al*. A whiff of oxygen before the Great Oxidation Event? *Science* **317,** 1903–1906 (2007).
5. Frei, R., Gaucher, C., Poulton, S. & Canfield, D. E. Fluctuations in Precambrian atmospheric oxygenation recorded by chromium isotopes. *Nature* **461,** 250–253 (2009).
6. Planavsky, N. J., Bekker, A., Rouxel, O. & Lyons, T. W. Iron isotope composition of some Archean and Proterozoic iron formations. *Geochim. Cosmochim. Acta* **80,** 158–169 (2012).
7. Kendall, B. *et al*. Pervasive oxygenation along late Archaean ocean margins. *Nat. Geosci.* **3,** 647–652 (2010).
8. Crowe, S. A. *et al*. Atmospheric oxygenation three billion years ago. *Nature* **501,** 535–538 (2013).
9. Kamber, B. S. Archean mafic-ultramafic oceanic landmasses and their effect on ocean-atmosphere chemistry. *Chem. Geol.* **274,** 19–28 (2010).
10. Kasting, J. F. What caused the rise of atmospheric $O_2$? *Chem. Geol.* **362,** 13–25 (2013).
11. Lee, C.-T. *et al*. Two-step rise of atmospheric oxygen linked to the growth of continents. *Nat. Geosci.* **9,** 417–424 (2016).
12. Konhauser, K. O. *et al*. Oceanic nickel depletion and a methanogen famine before the Great Oxidation Event. *Nature* **458,** 750–753 (2009).
13. Condie, K. C. *Earth as an Evolving Planetary System* Ch. 2, 1st edn, 11–58 (Elsevier, 2005).
14. Tang, M., Chen, K. & Rudnick, R. L. Archean upper crust transition from mafic to felsic marks the onset of plate tectonics. *Science* **351,** 372–375 (2016).
15. Kamber, B. The evolving nature of terrestrial crust from the Hadean, through the Archean, into the Proterozoic. *Precambrian Res.* **258,** 48–82 (2015).
16. Nutman, A. P. On the scarcity of >3900 Ma detrital zircons in >3500 Ma metasediments. *Precambrian Res.* **105,** 93–114 (2001).
17. Hawkesworth, C. J. *et al*. The generation and evolution of the continental crust. *J. Geol. Soc. Lond.* **167,** 229–248 (2010).
18. McLennan, S. M. & Taylor, S. R. Th and U in sedimentary rocks: crustal evolution and sedimentary recycling. *Nature* **285,** 621–624 (1980).
19. Taylor, S. R. & McLennan, S. M. The geochemical evolution of the continental crust. *Rev. Geophys.* **33,** 241–265 (1995).
20. Garçon, M. *et al*. Erosion of Archean continents: the Sm–Nd and Lu–Hf isotopic record of Barberton sedimentary rocks. *Geochim. Cosmochim. Acta* **206,** 216–235 (2017).
21. Rosing, M. T. & Frei, R. U-rich Archaean sea-floor sediments from Greenland indications of >3700 Ma oxygenic photosynthesis. *Earth Planet. Sci. Lett.* **217,** 237–244 (2004).
22. Oze, C., Bird, D. & Fendorf, S. Genesis of hexavalent chromium from natural sources in soil and groundwater. *Proc. Natl Acad. Sci. USA* **104,** 6544–6549 (2007).
23. Dhuime, B., Wuestefeld, A. & Hawkesworth, C. J. Emergence of modern continental crust about 3 billion years ago. *Nat. Geosci.* **8,** 552–555 (2015).

24. Næraa, T. *et al*. Hafnium isotope evidence for a transition in the dynamics of continental growth 3.2 Gyr ago. *Nature* **485,** 627–630 (2012).
25. Flament, N., Coltice, N. & Rey, P. F. A case for late-Archean continental emergence from thermal evolution models and hypsometry. *Earth Planet. Sci. Lett.* **275,** 326–336 (2008).
26. Heubeck, C. & Lowe, D. R. Depositional and tectonic setting of the Archean Moodies Group, Barberton Greenstone Belt, South Africa. *Precambrian Res.* **68,** 257–290 (1994).
27. Kröner, A. & Compston, W. Ion microprobe ages of zircons from early Archean granite pebbles and greywacke, Barberton Greenstone Belt, Southern Africa. *Precambrian Res.* **38,** 367–380 (1988).
28. Frei, R. *et al*. Oxidative elemental cycling under the $O_2$ Eoarchean atmosphere. *Sci. Rep.* **6,** 21058 (2016).
29. Planavsky, N. J. *et al*. Evidence for oxygenic photosynthesis half a billion years before the Great Oxidation Event. *Nat. Geosci.* **7,** 283–286 (2014).
30. Cottrell, E. & Kelley, K. A. The oxidation state of Fe in MORB glasses and the oxygen fugacity of the upper mantle. *Earth Planet. Sci. Lett.* **305,** 270–282 (2011).
31. Sleep, N. H., Meibom, A., Fridriksson, T., Coleman, R. G. & Bird, D. K. $H_2$-rich fluids from serpentinization: geochemical and biotic implications. *Proc. Natl Acad. Sci. USA* **101,** 12818–12823 (2004).
32. Frost, B. R. & Beard, J. S. On silica activity and serpentinization. *J. Petrol.* **48,** 1351–1368 (2007).
33. Berndt, M. E., Allen, D. E. & Seyfried, W. E. Reduction of $CO_2$ during serpentinization of olivine at 300 °C and 500 bar. *Geology* **24,** 351–354 (1996).
34. McCollom, T. M. & Seewald, J. S. A reassessment of the potential for reduction of dissolved $CO_2$ to hydrocarbons during serpentinization of olivine. *Geochim. Cosmochim. Acta* **65,** 3769–3778 (2001).
35. Schrenk, M. O., Brazelton, W. J. & Lang, S. Q. in *Carbon in Earth, Reviews in Mineralogy 75* (eds Hazen, R. M., Jones, A. P. & Baross, J. A.) 575–606 (Mineralogical Society of America, 2013).
36. Canfield, D. E. A new model for Proterozoic ocean chemistry. *Nature* **396,** 450–453 (1998).
37. Catling, D. C., Zahnle, K. J. & McKay, C. P. Biogenic methane, hydrogen escape, and the irreversible oxidation of early Earth. *Science* **293,** 839–843 (2001).
38. Kump, L. R. & Barley, M. E. Increased subaerial volcanism and the rise of atmospheric oxygen 2.5 billion years ago. *Nature* **448,** 1033–1036 (2007).


## Acknowledgements

Careful and constructive comments from P. R. D. Mason and M. Tang, as well as fruitful discussions with E. Kooijman, allowed us to improve the quality of the manuscript substantially. The research was financially supported by the Natural Sciences and Engineering Research Council of Canada, Discovery Grant RGPIN-2015-04080 to M.A.S.

## Author contributions

M.A.S. conceived the concepts, compiled and evaluated all data, designed the figures, and wrote the first draft manuscript. K.M. provided crucial topical insight and co-wrote the manuscript.

## Additional information

Supplementary information is available in the online version of the paper. Reprints and permissions information is available online at www.nature.com/reprints. Publisher's note: Springer Nature remains neutral with regard to jurisdictional claims in published maps and institutional affiliations. Correspondence and requests for materials should be addressed to M.A.S.

## Competing financial interests

The authors declare no competing financial interests.

## Methods

Data for Cr/U and $SiO_2$, as obtained from the GeoRoc database, were filtered for outliers per rock type by applying a $2\sigma$ outlier criterion for Cr/U. Averages and $2\sigma$ for $\Delta$(Cr/U) and CIPW-normative olivine content[39] were calculated for global rock reservoirs (data and references in Supplementary Table 1), combining all MORB and arc types in single populations. Standard error-weighted regression to estimate $\ln(ol_{CIPW})$ at $\Delta$(Cr/U) of 0 and $d\ln(ol_{CIPW})]/d\ \Delta$(Cr/U) was done using the Isoplot 3.75 statistical data evaluation package[40].

**Data availability.** The authors declare that the data supporting the findings of this study are available within the Supplementary Information files. The Cr/U data for global reservoirs and for the various shale occurrences are provided (with references) in Supplementary Tables 1 and 4, respectively. The Cr/U data for different rock types are available from the global GeoRoc database (georoc.mpch-mainz.gwdg.de/georoc) and are also provided with GeoRoc file names and download dates in Supplementary Fig. 2 and Supplementary Tables 2 and 3. All data are otherwise available in standard spreadsheet format upon request to the corresponding author.

## References

39. Kelsey, C. H. Calculation of the CIPW norm. *Mineral. Mag.* **34,** 276–282 (1965).
40. Ludwig, K. *Berkeley Geochron. Center Spec. Publ. 5* User's manual for Isoplot 3.75. 1–75 (Berkeley Geochronology Center, 2012).